

Application No.: 10/047,805

Docket No.: JCLA8069

**REMARKS****Present Status of the Application**

The Office Action rejected claims 1-6. Specifically, the Office Action rejected claims 1-6 under 35 U.S.C. 102(b) as being anticipated by Bergstedt (U. S. Patent 6,094,302). Alternatively, the Office Action also rejected claims 2 and 3 under 35 U.S.C. 103(a) as being unpatentable over Bergstedt. Applicants have amended independent claim 1 and cancelled claims 2-3. After entry of the foregoing amendments, claims 1 and 4-6 remain pending in the present application, and reconsideration of those claims is respectfully requested.

**Discussion of Office Action**

The Office Action rejected claims 1-6 under 35 U.S.C. 102(b) as being anticipated by Bergstedt. The Office Action also rejected claims 2 and 3 under 35 U.S.C. 103(a) as being unpatentable over Bergstedt. Applicants have amended independent claim 1 and respectfully traverse the rejections for at least the reasons set forth below.

With respect to amended independent claim 1, the first mirror and the third mirror are symmetric to the virtual reference surface, and their included angles are substantially equal to 60°. *The symmetric included angle at 60° is essential to achieve the de-rotation function.*

Application No.: 10/047,805

Docket No.: JCLA8069

Applicants submit the published paper in "2003 IEEE Carnahan Conference on Security Technology, p. 183-189", which is published by one of the inventors. In FIG. 13 of the published paper as discussed in Section 4.3, the three normal vectors N41, N42, and N43 are obtained. Then the whole reflection transfer matrix M4 can be diagonalized (page 9).

Therefore, the included angle by  $60^\circ$  is essential in de-rotation mechanism with the non-obviously unexpected result.

In re Bergstedt, the mirrors E, D, F are used in a camera. Basically, Bergstedt does not specifically consider the de-rotation function. More specifically, Bergstedt fails to disclose the included angle by  $60^\circ$ .

For at least the foregoing reasons, Applicants respectfully submit that independent claim 1 patently defines over the prior art, and should be allowed. For at least the same reasons, dependent claims 4-6 patently define over the prior art as well.

Application No.: 10/047,805

Docket No.: JCLA8069

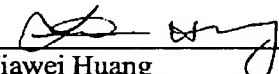
**CONCLUSIONS**

For at least the foregoing reasons, it is believed that all the pending claims 1 and 4-6 of the invention patently define over the prior art and are in proper condition for allowance. If the Examiner believes that a telephone conference would expedite the examination of the above-identified patent application, the Examiner is invited to call the undersigned.

Respectfully submitted,  
J.C. PATENTS

Date: 12/12/2003

4 Venture, Suite 250  
Irvine, CA 92618  
Tel.: (949) 660-0761  
Fax: (949) 660-0809

  
Jiawei Huang  
Registration No. 43,330

published in 2003 IEEE Carnahan Conference on  
Security Technology

## A Panoramic Stabilized Periscope With Common Optical Path P. 183-189

Ping-Ho Chen

Chief Engineer, Information and Communication Research Division, Chung-Shan Institute  
of Science and Technology, Taoyuan, Taiwan, ROC.

### Abstract

"Panoramic stabilization" and "common optical path" as designed in this paper are two significant issues regarding the technology of periscope detection. The idea of "panoramic stabilization" is to construct a pseudo level coordinate while in 360° searching. Sighting vector to the target expressed by spherical coordinate should be based on this panoramic stabilized level. The design of "common optical path" entirely employs a set of reflection mirrors with folded optical path for various light wave bands to shorten the size of the periscope. Devices associated with these features are developed and wrapped up in terms of an analysis of conceptual configuration. (Topic No. 2)

**Keyword:** Periscope, Panorama, Stabilization,  
Common optical path

### 1. Introduction

The paper relates to a periscope, and more particularly to a periscope having IR (infrared) rays, a laser beam and visible light going through the same optical path, being split by beam splitters and then being received by a CCD day sight camera, an IR night vision camera and a laser range finder (LRF).

Normally, military tanks are equipped with a periscope to gather useful information without risking exposure to personnel inside the vehicle. The periscope includes a CCD camera, an IR sight and a laser range finder, all of which have independent elements with respect to each other, and each has its own optical path. Therefore, the periscope is very large and expensive. Furthermore, due to the line of sight of each of the aforementioned elements, mounted on the same turret, being different from each other, the problem of over weighting, sighting parallax error, over sizing, and lag response caused by the turret might be crucial in modern warfare.

To overcome the shortcomings, this paper tends to provide an improved periscope to mitigate and obviate the aforementioned problems by integrating the different optical paths of the IR sight, the laser range finder and the CCD camera together so as to reduce the overall elements used in the periscope and the cost as well.

As shown in Fig. 1, the improved periscope [1] is composed of two portions, the upper portion and the lower portion physically. The upper portion, a portion of so-called common optical path, has a head mirror

assembly, a parabolic reflection mirror, an aspherical mirror and a de-rotation mirror module in sequence to shorten the common optical path in the periscope. The head mirror assembly, usually tilting at 45°, has two gimbals on which a head mirror, two PM motors [2], two gyroscopes and two resolvers are mounted. The parabolic reflection mirror reflects the light upward for folding the optical path. The aspherical mirror, mounted on a mechanism for controlling focusing and magnification [3], reflects the light downward. The de-rotation mirror module [4] de-rotates the image to compensate for the traverse azimuth (AZ) rotation between the periscope head and its body.

The lower portion is composed of beam splitters, lenses, reflecting mirrors for splitting the IR ray to IR camera and the visible light to CCD camera individually. Furthermore, employing a two-way polarized beam splitter allows the laser beam to be transmitted and received by the laser range finder. In this way, three different light beams are able to share a common optical path in the upper portion and to be split via beam splitters in the lower portion. Size and cost of the elements in the periscope are thus reduced.

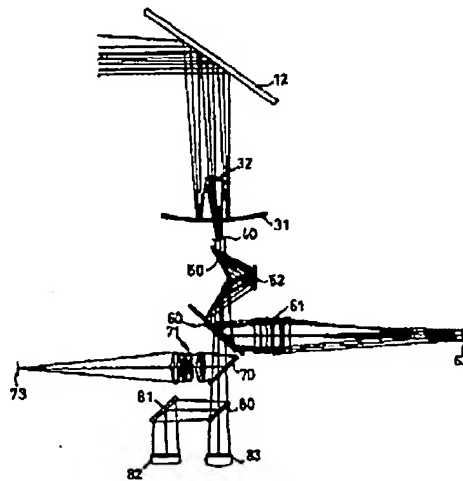


Fig. 1 A configuration of the periscope

As to the control function, "panoramic searching", "attitude stabilization" and "de-rotation" are three key issues to be improved and illustrated in the following. The purpose of panoramic searching is

to acquire a panoramic view with constant AZ rate and fix elevation (EL) angle relative to the level regardless of platform tilting or yawing motion. The function of stabilization for stabilizing the line of sight (LOS) is needed whenever there exists rate of platform tilting and yawing motion, or even the rate of target motion, and rate of level searching command.

## 2. Panoramic searching [5]

Since the head mirror of traditional periscope mounted on the turret usually has only an EL gimbal, the target acquisition is based on the AZ drive of gun turret. The periscope itself is unable to search for panorama independently and thus fails to record the panorama image and process it for automatic video tracking (AVT). For those periscopes to date, equipped with dual gimbal drive (AZ & EL), an approach to control the gimbal angle is developed as follows to have the light reflected from the head mirror align with the internal longitudinal optical path. Panoramic searching is to generate a 360° panorama via level searching by controlling the dual head mirror gimbals in cases of platform tilting and yawing. Note that the target search sighting vector, i. e. incident light vector to the head mirror, is defined in terms of level coordinate. The inputs while searching are 1) platform attitude angles heading, pitch and roll, 2) fix angle "E" w. r. t. the level and 3) angle "A" w. r. t. the level. The outputs are 1) head mirror AZ command 2) head mirror EL command

### 2.1 Geographic level coordinate

In the following approach, local level coordinate  $\langle E_L, N_L, U_L \rangle$  with " $E_L$ " denoting the east, " $N_L$ " the north and " $U_L$ " the vertical up is complied with the right hand rule as shown in Fig. 2. Heading angle "H" is along the vertical relative to the north. Pitch angle "P" is along the starboard axis. Roll angle "R" is along the longitudinal axis.

### 2.2 Gimbal tottem and notation

The mounting sequence of gimbal tottem in the drive mechanism of gyrocompasses or the head mirror of periscope is important whenever coordinate transformation is applied. Platform attitude "H", "P" and "R" relative to the geographic level coordinate is usually sensed by gyrocompasses or inertial navigators in which the gimbal tottem is a type of "H over P, P over R". As to the head mirror of periscope, the gimbal tottem is a type of "EL over AZ". Furthermore, the searching vector  $\langle A, E \rangle$  in spherical coordinate relative to the geographic level is a pseudo gimbal tottem of "E over A" type. The spatial /level searching format for constant speed search on level or fix EL search above level is given respectively by:

$$\dot{A} = \text{Const}, E = 0 \quad (1)$$

$$\dot{A} = \text{Const}, E > 0 \quad (2)$$

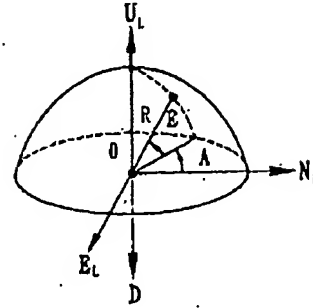


Fig.2 Local level coordinate

## 2.3 Coordinate transformation

Assume that the instant search angle is  $\langle A, E \rangle_s$ , the platform attitude angle is  $\langle H, P, R \rangle_a$ , the head mirror gimbal angle is  $\langle AZ, EL \rangle_m$ , where subscript "S" denotes the search, "G" the gyrocompass and "M" the head mirror, then the coordinate transformation is given as follows. As shown in Fig. 3, three unit vectors along the level coordinate  $\langle E, N, U \rangle_L$  are transformed to the head mirror gimbal coordinate  $\langle X_3, Y_3, Z_3 \rangle$  via the coordinate transformation sequence  $[H] \rightarrow [P] \rightarrow [R]$  defined by:

$$[H] = \begin{bmatrix} \cos H & \sin H & 0 \\ -\sin H & \cos H & 0 \\ 0 & 0 & 1 \end{bmatrix} \quad (3)$$

$$[P] = \begin{bmatrix} 1 & 0 & 0 \\ 0 & \cos P & \sin P \\ 0 & -\sin P & \cos P \end{bmatrix} \quad (4)$$

$$[R] = \begin{bmatrix} \cos R & 0 & \sin R \\ 0 & 1 & 0 \\ -\sin R & 0 & \cos R \end{bmatrix} \quad (5)$$

The three projected unit vectors  $e_{3,x}, e_{3,y}$  and  $e_{3,z}$  in  $\langle X_3, Y_3, Z_3 \rangle$  coordinate after  $[H] \rightarrow [P] \rightarrow [R]$  transformation are obtained as follows:

$$\textcircled{3} e_{3,x} = \begin{bmatrix} e_{x3,x} \\ e_{y3,x} \\ e_{z3,x} \end{bmatrix} = [R][P][H] \begin{bmatrix} 1 \\ 0 \\ 0 \end{bmatrix} \quad (6)$$

$$e_{3,y} = \begin{bmatrix} e_{x3,y} \\ e_{y3,y} \\ e_{z3,y} \end{bmatrix} = [R][P][H] \begin{bmatrix} 0 \\ 1 \\ 0 \end{bmatrix} \quad (7)$$

$$e_{3,z} = \begin{bmatrix} e_{x,z} \\ e_{y,z} \\ e_{z,z} \end{bmatrix} = [R][P][H] \begin{bmatrix} 0 \\ 0 \\ 1 \end{bmatrix} \quad (8)$$

$$\begin{bmatrix} e_{3,x} & e_{3,y} & e_{3,z} \end{bmatrix} = [R][P][H] \begin{bmatrix} 1 & 0 & 0 \\ 0 & 1 & 0 \\ 0 & 0 & 1 \end{bmatrix} \quad (9)$$

$$\begin{bmatrix} e_{3,x} & e_{3,y} & e_{3,z} \end{bmatrix} = [R][P][H] \quad (10)$$

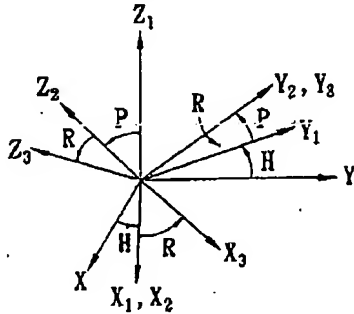


Fig.3 [R][P][H] coordinate transformation

## 2.4 Angular command of head gimbal

Assuming at the  $N$ 'th time increment, the level search angle is  $A_N$ , then the search unit vector  $e_{AN}$  on the level is

$$e_{AN} = \begin{bmatrix} -\sin A_N \\ \cos A_N \\ 0 \end{bmatrix} \quad (11)$$

As shown in Fig.4, the projection  $X_{3,AN}$ ,  $Y_{3,AN}$  and  $Z_{3,AN}$  on the  $\langle X_3, Y_3, Z_3 \rangle$  respectively from the search unit vector  $e_{AN}$  is calculated as follows:

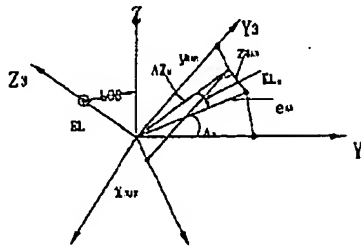


Fig.4 Projection from search level to head gimbal

$$\begin{bmatrix} X_{3,AN} \\ Y_{3,AN} \\ Z_{3,AN} \end{bmatrix} = \begin{bmatrix} e_{3,x} & e_{3,y} & e_{3,z} \end{bmatrix} e_{AN} \quad (12)$$

Where  $\begin{bmatrix} e_{3,x} & e_{3,y} & e_{3,z} \end{bmatrix}$  is a  $3 \times 3$  matrix.

Normalize

$$x_{3,AN}^2 + y_{3,AN}^2 + z_{3,AN}^2 = k^2 \quad (13)$$

$$\bar{x}_{3,AN} = x_{3,AN} / k \quad (14)$$

$$\bar{y}_{3,AN} = y_{3,AN} / k \quad (15)$$

$$\bar{z}_{3,AN} = z_{3,AN} / k \quad (16)$$

The gimbal angular commands are

$$AZ_{AN} = \tan^{-1} (\bar{y}_{3,AN} / \bar{x}_{3,AN}) \quad (17)$$

$$EL_{AN} = \tan^{-1} (\bar{z}_{3,AN} / \sqrt{\bar{x}_{3,AN}^2 + \bar{y}_{3,AN}^2}) \quad (18)$$

After the drive control of gimbal  $AZ_{AN}$ , the three

vectors  $Z_3$ ,  $\langle x_{3,AN}, y_{3,AN} \rangle$  and  $e_{AN}$  remain on the same plane. Moreover, after the drive control of gimbal  $EL_{AN}$ , the head mirror sighting vector and  $e_{AN}$  are parallel and on the same plane as required.

## 3. Attitude stabilization [6]

A control method for attitude stabilization applied to the periscope, said method is a combination application of a coordinate transformation, a gyroscope and an automatic video processing to obtain panoramic stabilization of periscope in the operation modes of "searching", "tracking" and "firing".

### 3.1 Searching stabilization

The operation of searching mode is based on a level spherical coordinate system so that head mirror sighting vector is scanned at constant velocity orthogonal to the level. Without stabilization, sighting vector of head mirror will be affected by platform attitude angle rate, i.e. heading rate, pitching rate and yawing rate. Therefore, attitude stabilization plays a significant role while searching since head mirror sighting vector should be stabilized on the level or at a fixed EL angle above the level so as to keep the reflected light remain on the optical path inside the periscope as if it were stationary regardless of platform attitude change rate.

The design of attitude stabilization is to scheme the control of the shafts of head mirror motors rather than that of head mirror in cases of platform tilting or yawing while searching. Note that the shaft of head mirror EL motor is linked to that of head mirror by a mechanism as shown in Fig. 5. With reference to Fig. 5, it illustrates the stabilization theory of head mirror and elevation motor shaft while the platform being tilted. For stationary surface target, LOS (line of sight) is certainly on the level and the platform plane or the platform normal line vertical is assumed to pitch up an angle  $\theta$  to LOS in CCW direction along the EL axis. In the meanwhile, head mirror M accordingly also pitches up an angle  $\theta$  to M' in CCW direction. It will result in that the reflected light of head mirror pitches up  $2\theta$  from the local vertical or  $\theta$  from the platform normal line. In order to have the reflected light of head mirror remain on the platform normal line, M' should be rotated back an angle  $\theta/2$  in CW direction to M'' by controlling the angle of head mirror EL motor as

DEC-10-2003 WED 11:20

JCPO Taiwan

FAX NO. 886 2 2369 8454

P. 05/08

indicated by the new mirror normal line  $N'$ . In other words, the amplitude of counter rotation of head mirror is just half of the platform pitch angle. Furthermore, EL motor is to rotate an angle  $\theta$  in CW direction wherein the gear ratio of motor axis to head mirror is 1:2 and the angle reading  $\theta$  from the resolver mounted on EL motor shaft is thus the so-called stabilization angle.

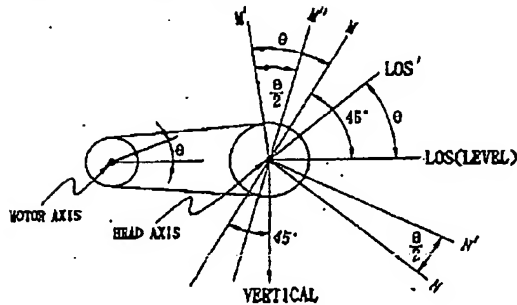


Fig. 5 EL stabilization

As aforementioned, the generalized attitude stabilization is just regarding the angle compensation associated with the coordinate transformation. But for rugged stabilization, compensation of angular rate or even angular acceleration is also required. In Fig. 6, EL stabilization loop is operated by employing a rate integrating gyroscope of closed loop to sense the EL inertial rate of the shaft of head mirror EL motor so as to compensate for the rate of platform tilting composed of pitch and roll. As to the AZ stabilization, it is straight to construct the control loop via the above concept of the EL stabilization.

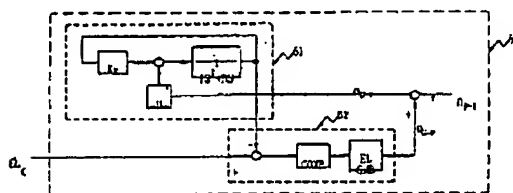


Fig. 6 EL stabilization loop

### 3.2 tracking stabilization

Fig. 7 illustrates the tracking stabilization of head mirror and its EL drive motor. Assuming that the platform is stationary while the target is moving up, then LOS pitches up an angle, said  $\Phi$ , in CCW direction to the LOS' in the sense. Without control of head mirror, the light reflected from head mirror rotates  $\Phi$  in CW direction from the platform normal line or the vertical. In order to have the light reflected from head mirror still stay on the platform normal line, the head mirror has to rotate  $\Phi/2$  in CCW with normal line  $N$  rotating to  $N'$ . In other words, EL motor has to rotate  $\Phi$  in CCW direction through the 1:2 mechanism. Obviously, the motor angle to be

controlled is equivalent to the LOS angle  $\Phi$  and the reading of  $\Phi$  is picked up from the EL resolver.

In cases of presenting both platform tilting  $\theta$  and target tracking  $\Phi$ , the combined control angle of the EL motor from attitude stabilization and tracking stabilization will be  $\Phi - \theta$ . This result points out that the amplitude of compensation control is the same as that of the sensing if employing the 1:2 mechanism. In this way, the so-called "half angle reflection" as above is no more a trouble problem to the control design.

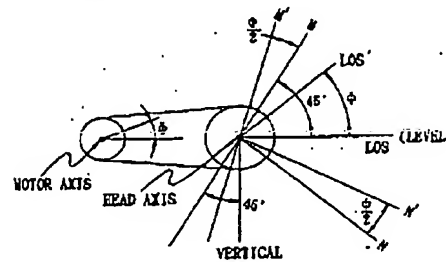


Fig. 7 EL tracking loop

Fig. 8(a) shows a block diagram of tracking stabilization, and Fig. 8(b) a complementary weighting rate assignment, i.e. weighting factors of stabilization  $W_s$  and tracking  $W_t$  w. r. t. tracking error. Note that in Eq. (19) and (20),  $\theta_{T-I}$  and  $\dot{\theta}_{T-I}$  are two states to be controlled.

$$\theta_{T-I} = \theta_{T-G} + \theta_{G-P} + \theta_{P-I} \quad (19)$$

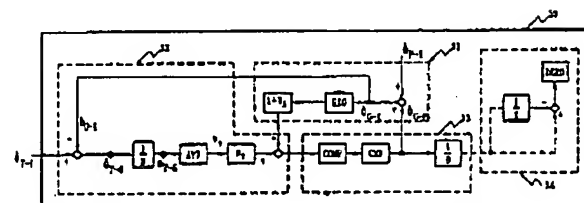
$$\dot{\theta}_{T-I} = \dot{\theta}_{T-G} + \dot{\theta}_{G-P} + \dot{\theta}_{P-I} = \dot{\theta}_{T-G} + \dot{\theta}_{G-I} \quad (20)$$

Where

$$\text{tracking error } \varepsilon = \theta_{T-G}$$

$$\text{rate of tracking error } \dot{\varepsilon} = \dot{\theta}_{T-G}$$

(T : Target, I : Inertia, G : Gimbal, P : Platform)



(a)



(b)

Fig. 8. A loop of tracking stabilization

In Fig. 8,  $W_T$  and  $W_S$  are complementary given by:

$$W_T + W_S = 1 \quad (21)$$

The other notations are defined as follows:

AVT: Automatic video tracking, RIG: Rate integration gyroscope, COMP: Compensator, GMB: Gimbal, DERO: De-rotation,  $W_s$ : Weighting factor of stabilization,  $W_T$ : Weighting factor of tracking, 31: Gyro stabilization, 32: Video tracking, 33: Gimbal servo, 34: De-rotation (only for AZ gimbal)

### 3.3 Firing stabilization

In Fig. 9, a sequence of LOS, i.e. LOS 1, LOS 2 and LOS 3 to the right, is shown to illustrate the firing stabilization. The traditional firing procedure has two phases, i.e. lay-on-target and relay-on-target. At the instant of LOS 1 during the phase of lay-on-target, calculation of leading angle  $\theta_L$  to the right is completed and the reticle is pulled off  $\theta_L$  to the left by AVT. During the short duration that the gun rotates  $\theta_L$  to the right w. r. t. LOS 2, the target moves  $\Delta\theta$  from LOS 1 to LOS 2 in the sense of traditional relay-on-target. In other words, the gun totally moves  $\theta_L + \Delta\theta$  to LOS 3 or LOF, the line of fire. In the mean time, the reticle also moves  $\theta_L + \Delta\theta$  to LOS 2. In this way, the traditional manual modes of lay-on-target and relay-on-target are automatically accomplished by gyro stabilization firing computer and image processing AVT.

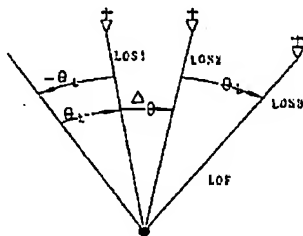


Fig.9 LOS and firing stabilization

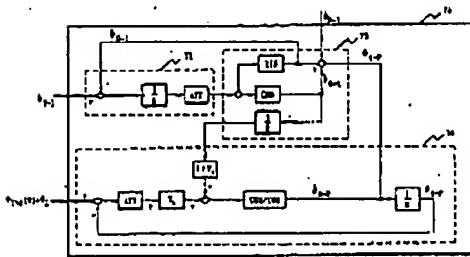


Fig. 10 A loop of firing stabilization

Fig. 10 shows the loop of firing stabilization still using the complementary approach, wherein including:

71: Video processing, 72: Gimbal stabilization, 73: Gun control, AVT: Automatic video tracking, RIG: Rate integrating gyroscope, GMB: Gimbal,  $W_k$ : Relay weighting factor,  $W_L$ : Lay weighting factor, GUN/TUR: Gun/Turret Note that

$$W_k + W_L = 1 \quad (22)$$

### 4. De-rotation [7]

In order to keep the vertical polarity of acquired image in the periscope from disturbing of the head mirror AZ rotation, a de-rotation mechanism has to be designed so as to compensate for the traverse rotation caused by the head mirror AZ rotation.

#### 4.1 Reflection matrix

Fig. 11 shows an input object with  $\langle P, R, U \rangle$  vector, where " $P$ " is the incident light vector to the mirror and " $R$ " to the object right, " $U$ " to the object upper as viewed from the normal vector  $N$  of the mirror plane  $M_p$ .

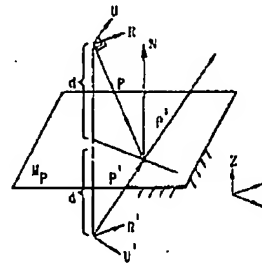


Fig.11 Mirror reflection

Obviously

$$R \perp P, R \perp U, U \perp P, P = U \times R, R \parallel M_p \quad (23)$$

Assuming that  $R^1$  is the right vector of the reflected image and  $U^1$  the upper one. There exists a reflection matrix " $M$ " to transfer from the incident light vector " $P$ " to the reflected light " $P^1$ " and so on such that:

$$P^1 = MP \quad (24)$$

$$R^1 = MR \quad (25)$$

$$U^1 = MU \quad (26)$$

Assuming

$$N = \begin{bmatrix} N_x \\ N_y \\ N_z \end{bmatrix}, P = \begin{bmatrix} P_x \\ P_y \\ P_z \end{bmatrix}, P^1 = \begin{bmatrix} P^1_x \\ P^1_y \\ P^1_z \end{bmatrix} \quad (27)$$

Then we have



$$M = \begin{bmatrix} (1-2N_x^2) - 2N_xN_y - 2N_xN_z \\ -2N_xN_y(1-2N_y^2) - 2N_yN_z \\ -2N_xN_z - 2N_yN_z(1-2N_z^2) \end{bmatrix} \quad (28)$$

#### 4.2 Effect of head mirror AZ rotation

Assuming the head mirror AZ gimbal is originally fixed with mirror normal  $N$ , tilted to  $45^\circ$  below the level as shown in Fig.12. Then we have

$$N = \frac{1}{\sqrt{2}} \begin{bmatrix} -1 \\ 0 \\ -1 \end{bmatrix}_{(x,y,z)} \quad (29)$$

$$\Rightarrow [P_{10}R_{10}U_{10}] = [I - 2N_1N_1^T][P_{1i}R_{1i}U_{1i}] \quad (30)$$

Note that the subscript "i" means the input, "0" the output and

$$M_1 = I - 2N_1N_1^T \quad (31)$$

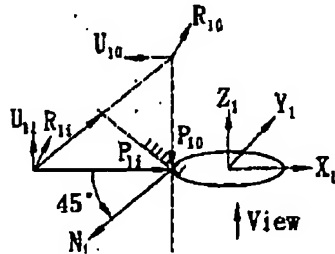


Fig.12 Head mirror reflection

Whenever head mirror AZ rotates  $\theta$  angle, the new normal vector  $N_{1\theta}$  is

$$N_{1\theta} = R_\theta N_1 \quad (R_\theta \text{ is rotation matrix}) \quad (32)$$

$$= \begin{bmatrix} \cos\theta & -\sin\theta & 0 \\ \sin\theta & \cos\theta & 0 \\ 0 & 0 & 1 \end{bmatrix} \left( \frac{1}{\sqrt{2}} \begin{bmatrix} -1 \\ 0 \\ -1 \end{bmatrix} \right) \quad (33)$$

$$= \frac{1}{\sqrt{2}} \begin{bmatrix} -\cos\theta \\ -\sin\theta \\ -1 \end{bmatrix} \quad (34)$$

Since rotation matrix is orthogonal, we have

$$[P_{10}R_{10}U_{10}] = R_\theta (I - 2N_1N_1^T) R_\theta^T [P_{1i}R_{1i}U_{1i}] \quad (35)$$

$$M_{1\theta} = R_\theta (I - 2N_1N_1^T) R_\theta^T \quad (36)$$

$$\text{i.e. } M_{1\theta} = R_\theta M_1 R_\theta^T \quad (37)$$

$$= \begin{bmatrix} \cos\theta & -\sin\theta & 0 \\ \sin\theta & \cos\theta & 0 \\ 0 & 0 & 1 \end{bmatrix} \begin{bmatrix} 0 & 0 & -1 \\ 0 & 1 & 0 \\ -1 & 0 & 0 \end{bmatrix} \begin{bmatrix} \cos\theta & \sin\theta & 0 \\ -\sin\theta & \cos\theta & 0 \\ 0 & 0 & 1 \end{bmatrix} \quad (38)$$

$$= \begin{bmatrix} \sin^2\theta & -\sin\theta\cos\theta & -\cos\theta \\ -\sin\theta\cos\theta & \cos^2\theta & -\sin\theta \\ -\cos\theta & -\sin\theta & 0 \end{bmatrix} \quad (39)$$

The right column indicates that the vertical polarity is tilted to an angle  $\theta$  in the fourth quadrant of  $\langle X_1, Y_1 \rangle$  plane. After next two reflections via parabolic mirror and aspherical mirror, the vertical polarity is rotated to the first quadrant of  $\langle X_3, Y_3 \rangle$  plane.

#### 4.3 De-rotation transfer matrix

As shown in Fig.13, the de-rotation mechanism is composed of three reflection mirrors with normal lines mutually separated by  $120^\circ$  and expressed by:

$$N_{41} = \begin{bmatrix} -\sqrt{3}/2 \\ 0 \\ 1/2 \end{bmatrix}, N_{42} = \begin{bmatrix} 1 \\ 0 \\ 0 \end{bmatrix}, N_{43} = \begin{bmatrix} -\sqrt{3}/2 \\ 0 \\ -1/2 \end{bmatrix} \quad (40)$$

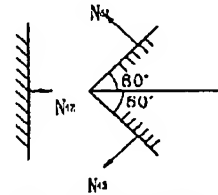


Fig.13 De-rotation mirror module

Each reflection transfer matrix  $M_{4i}$  ( $i=1,2,3$ ) is expressed by:

$$M_{41} = I - 2N_{41}N_{41}^T \quad (41)$$

$$M_{42} = I - 2N_{42}N_{42}^T \quad (42)$$

$$M_{43} = I - 2N_{43}N_{43}^T \quad (43)$$

Sub. Eq.(40) into Eq.(41),(42)and (43)

$$M_{41} = \begin{bmatrix} -1/2 & 0 & \sqrt{3}/2 \\ 0 & 1 & 0 \\ \sqrt{3}/2 & 0 & 1/2 \end{bmatrix}, M_{42} = \begin{bmatrix} -1 & 0 & 0 \\ 0 & 1 & 0 \\ 0 & 0 & 1 \end{bmatrix}, M_{43} = \begin{bmatrix} -1/2 & 0 & -\sqrt{3}/2 \\ 0 & 1 & 0 \\ -\sqrt{3}/2 & 0 & 1/2 \end{bmatrix} \quad (44)$$

The whole reflection transfer matrix  $M_4$  is

$$M_4 = M_{43}M_{42}M_{41} = \begin{bmatrix} -1 & 0 & 0 \\ 0 & 1 & 0 \\ 0 & 0 & 1 \end{bmatrix} \quad (45)$$

Eq.(45) points out that the vertical polarity is now rotated to the second quadrant as shown in Fig.14 without de-rotation compensation. Suppose that de-

rotation module is rotated  $\Phi$  along the  $Z_4$  axis, the vertical polarity will move to the negative  $X_4$ . The de-rotation effect is thus eliminated. Then we have

$$M_{4\Phi} = R_{\Phi} M_4 R_{\Phi}^T \quad (46)$$

Where

$$R_{\Phi} = \begin{bmatrix} \cos\phi & \sin\phi & 0 \\ -\sin\phi & \cos\phi & 0 \\ 0 & 0 & 1 \end{bmatrix} \quad (47)$$

$$m \begin{bmatrix} -1 \\ 0 \\ 0 \end{bmatrix} = \begin{bmatrix} \cos\phi & \sin\phi & 0 \\ -\sin\phi & \cos\phi & 0 \\ 0 & 0 & 1 \end{bmatrix} \begin{bmatrix} -1 & 0 & 0 \\ 0 & 1 & 0 \\ 0 & 0 & 1 \end{bmatrix} \begin{bmatrix} \cos\phi & -\sin\phi & 0 \\ \sin\phi & \cos\phi & 0 \\ 0 & 0 & 1 \end{bmatrix} \begin{bmatrix} m\cos\phi \\ m\sin\phi \\ 0 \end{bmatrix} \quad (48)$$

reflection mirror. We obtain Where "m" is the magnification of parabolic

$$\phi = -\frac{\theta}{2} \quad (49)$$

Eq. (49) indicates that the de-rotation control angle is counter half of the head mirror AZ rotation angle.

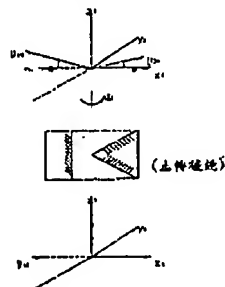


Fig.14 Input and output of de-rotation module

## 5. Conclusion

A configuration design of the panoramic stabilized periscope with common optical path is developed in this paper. Three significant issues, i.e. "panoramic searching", "attitude stabilization" and "image de-rotation" are analyzed respectively. Based on the approaches given above, following research associated with "de-rotation simulation", "panel display for modes of searching and stabilization" and "implementation hardware" are further accomplished without illustrated due to page limitation.

## Reference

1. Ping-Ho Chen et al. "Periscope using common optical path to have stabilized panoramic view", US patent No. US 6,347,010 B1, Feb.12, 2002.
2. Ping-Ho Chen; "Multiple layer double rotor single stator skew symmetry PM motor", US patent No. US 6,455,969 B1, Sep. 24, 2002.
3. Ping-Ho Chen et al. "Field-of-view switching and focusing system of common optical path periscope", ROC Taiwan patent approved notice No. 514747, Nov. 2002.

4. Lian Tongshu; "Theory of Conjugation for Reflecting Prisms", International Academic Publishers, 1991.
5. Ping-Ho Chen; "A control scheme of spatial and level searching applied to a panoramic stabilized periscope", US patent in application. Nov. 2002.
6. Ping-Ho Chen; "A panoramic stabilized control scheme applied to a common optical path periscope", US patent in application. Nov. 2002.
7. Ping-Ho Chen et al. "A design of the de-rotation mechanism in a common optical path panoramic stabilized periscope", ROC Taiwan patent approved No. 514746, Nov. 2002.